Journal of Pharmacognosy and Phytochemistry

Available online at www.phytojournal.com

E-ISSN: 2278-4136
P-ISSN: 2349-8234
www.phytojournal.com
JPP 2020; 9(6): 08-18
Received: 12-09-2020
Accepted: 18-10-2020

Abisola Ave-Maria Olushola-Siedoks
Department of Chemical, Fibre and Environmental Technology, Federal Institute of Industrial Research, Oshodi. 3, FIIRO road, Agege Motor road, Oshodi, Lagos, Nigeria, 21023

Ukachi Ezinna Igbo
Department of Chemical, Fibre and Environmental Technology, Federal Institute of Industrial Research, Oshodi. 3, FIIRO road, Agege Motor road, Oshodi, Lagos, Nigeria, 21023

Godfrey Asieba
Department of Production, Analytical and Laboratory Management, Federal Institute of Industrial Research, Oshodi. 3, FIIRO road, Agege Motor road, Oshodi, Lagos, Nigeria, 21023

Ibilola Adiza Damola
Department of Production, Analytical and Laboratory Management, Federal Institute of Industrial Research, Oshodi. 3, FIIRO road, Agege Motor road, Oshodi, Lagos, Nigeria, 21023

Chima Cartney Igwe
Department of Chemical, Fibre and Environmental Technology, Federal Institute of Industrial Research, Oshodi. 3, FIIRO road, Agege Motor road, Oshodi, Lagos, Nigeria, 21023

Corresponding Author:
Abisola Ave-Maria Olushola-Siedoks
Department of Chemical, Fibre and Environmental Technology, Federal Institute of Industrial Research, Oshodi. 3, FIIRO road, Agege Motor road, Oshodi, Lagos, Nigeria, 21023

GC-MS aided *In silico* molecular docking studies on the anti-sickling properties of *Zanthoxylum zanthoxyloides* (Lam.) Zepern. & Timler stem bark

Abisola Ave-Maria Olushola-Siedoks, Ukachi Ezinna Igbo, Godfrey Asieba, Ibilola Adiza Damola and Chima Cartney Igwe

DOI: https://doi.org/10.22271/phyto.2020.v9.i6a.12903

Abstract
Zanthoxylum zanthoxyloides is an important medicinal herb in African traditional medicine. It has been used to treat an array of pathological conditions, most notably is sickle cell anaemia, one of the most important genetic haematological conditions affecting individuals of African descent. This study identifies and evaluates *Zanthoxylum zanthoxyloides* bioactives with potential haemoglobin oxygen-affinity modulatory activity. Phytochemical constituents identified via gas chromatography-mass spectrometry of a 70% ethanolic stem bark extract of *Zanthoxylum zanthoxyloides* (Lam.) Zepern. and Timler were analyzed for their *in silico* anti-sickling activity. Gas chromatography-mass spectrometry aided *in silico* molecular docking studies identified the presence of two compounds, 7-(dimethylamino)-2,3-dihydro-1H cyclopenta[c]chromen-4-one and (8S,9S,10R,13S,14S,16R,17S)-17-acetyl-6,10,13,16-tetramethyl-8,9,11,12,14,15,16,17-octahydrocyclopenta[a]phenanthren-3-one, with a strong binding affinity for the active pocket located at the N-terminal region (valine 1) of the alpha globin subunit of haemoglobin S. Further analysis of the binding pose of the ligands demonstrated the formation of favourable interactions including hydrogen bonding, π-cation, van der Waals and hydrophobic contacts. Computational investigations on the pharmacokinetic profile of 7-(dimethylamino)-2,3-dihydro-1H cyclopenta[c]chromen-4-one and (8S,9S,10R,13S,14S,16R,17S)-17-acetyl-6,10,13,16-tetramethyl-8,9,11,12,14,15,16,17-octahydrocyclopenta[a]phenanthren-3-one reveals a favourable oral bioavailability and drug-likeness profile. The findings add to the evidence bolstering the role of *Zanthoxylum zanthoxyloides* in the management of sickle cell anemia.

Keywords: Sickle cell anaemia, *Zanthoxylum zanthoxyloides*, GC-MS, Molecular docking, Haemoglobin oxygen-affinity modulatory activity

1. Introduction
Sickle cell anaemia is a major public health challenge in Africa. It is a hereditary haemoglobinopathy characterized by the production of defective haemoglobin A and, in recent times, there has been a boom in the research and development of therapies to prevent, diagnose, manage and cure this condition [1]. The mechanisms of action being employed to ameliorate the cascade of events that results in the clinical manifestations of sickle cell anemia include induction/ of foetal haemoglobin expression, increase in nitric oxide bioavailability, reduction in circulating inflammatory mediators and\or their activity [2], regulation of adenosine levels [3], reduction in oxidative stress, regulation of the redox potential of nicotinamide adenine dinucleotide [4], inhibition of sickle haemoglobin (Hb S) polymerization, pan-selectin inhibition, p-selectin and interleukin-1β antibody reaction, inhibition of coagulation factor Xa and other coagulative activity, cell adhesion molecule inhibition, hematopoietic cell therapy, phosphodiesterase 9 inhibition, soluble guanylate cyclase stimulation, platelet activation inhibition and gene therapy [5, 6].
The inhibition of Hb S polymerization acts at a primary pathophysiological step of sickle cell anemia and has been steadily gaining traction. This mechanism of action involves the prevention of the formation of hydrophobic contacts and other pathological interactions between deoxygenated Hb S tetramers. Residues implicated in the polymerization of Hb S tetramers to form spindles include the substituted valine-6 on the beta Hb S subunit and phenylalanine-85 and leucine-88 at an acceptor pocket on the beta subunit of the adjacent Hb S tetramer. This interaction has been demonstrated to be involved in the initial step of Hb S polymerization. Further aggregation between these deoxygenated Hb S tetramers ultimately leads to the formation of multiple rigid long helical strands[7]. The Hb S polymerization inhibitors have been demonstrated to inhibit the polymerization sequalae by allosteric

modulatory activity which results in a conformational change in the quaternary Hb S structure from a low oxygen-affinity deoxygenated (T-state) Hb S to a high oxygen-affinity oxygenated (R-state) Hb S resulting in a shift of the oxygen dissociation curve to the left favouring the high oxygen-affinity oxygenated state of Hb S. These compounds are also known as haemoglobin oxygen-affinity modulators. They have been demonstrated via x-ray crystallographic experiments to act by binding at the N-terminal valine (Valine 1) on the alpha subunit of Hb S tetramers through Schiff-base, non-covalent polar and hydrophobic intermolecular interactions to stabilize the R-state of haemoglobin, which increases the affinity of haemoglobin for oxygen and destabilizes Hb S fibre formation [8]. With the elucidation of the mechanism of action at the molecular level, the *in-silico* approach to identify compounds with haemoglobin oxygen-affinity modulatory activity is viable.

Zanthoxylum zanthoxyloides plant has been historically used in African traditional medicine for the management of sickle cell anemia and several commercial products, notably FACA and Depranostat, containing *Zanthoxylum zanthoxyloides* have been launched into the pharmaceutical market [9]. However, there is a dearth of data on the active phytochemicals and the mechanism of action responsible for the reported anti-sickling properties of *Zanthoxylum zanthoxyloides*. There are studies linking the pharmacological properties of *Z. zanthoxyloides* in sickle cell anemia to a series of phenolic acids including vanillic acid, hydroxybenzoic acid, 2-hydroxymethyl benzoic acid, para-fluorobenzoic acid as well as three divanilloylquinic acid isomers [10-12].

The present study is designed to identify and evaluate potential haemoglobin oxygen-affinity modulatory activity of phytochemicals found in *Zanthoxylum zanthoxyloides* utilizing *in silico* tools; molecular docking and ADME prediction.

2. Materials and Methods

2.1 Protein Structure Preparation: The crystal structure of liganded carbonmonoxy haemoglobin S (PDB ID: 5E83) was retrieved from the Protein Data Bank (http://www.rcsb.org/structure/5E83) [13]. The ligand, 2-methyl-3-({2-[1-(propan-2-yl)-1H-pyrazol-5-yl]pyridin-3-yl}methoxy)phenol, water molecules and other associated solvent molecules were removed from the structure using BIOVIA Discovery Studio visualizer [14]. Utilizing AutoDock Tools (ADT) software version 1.5.6 [15], polar hydrogens, Kollman united atom charges and atomic solvation parameters were added. Non-polar hydrogens were merged. ADT was used to generate the docking input file, PDBQT file. The protein was docked as a rigid model structure and no relaxation of the protein was performed.

2.2 Ligand Structure Preparation: The ligands for this study were selected from the GC-MS total ion chromatogram (TIC) peak report of our previous investigations on the chemical constituents in 70% ethanolic *Z. zanthoxyloides* stem bark extract [16]. Their 3D structure was downloaded from National Center for Biotechnology Information, PubChem Database [17]. Using Chimera UCSF software [18], the downloaded SDF ligand files with all hydrogens included were converted to PDB file format. With ADT, the Gasteiger charges were added and non-polar hydrogens were merged while aromatic carbons, rigid roots and rotatable bonds were detected. The files were then saved as the PDBQT file format for docking. The ligands were allowed torsional freedom to permit exhaustive orientation and conformational possibility.

2.3 Active site and grid generation: A grid enclosing the reported binding site of haemoglobin affinity modulators, in the vicinity of the N-terminal (valine1) of the alpha subunit of the Hb S protein was defined. The co-crystallized ligand, 2-methyl-3-({2-[1-(propan-2-yl)-1H-pyrazol-5-yl]pyridin-3-yl}methoxy)phenol, was also bound to residues at this site. The grid box dimensions for the X, Y and Z axis were set at 126, 126 and 126 respectively with a spacing of 0.375 angstrom between grid points. The center grid box for x, y and z was defined at 20, 5 and 20, respectively.

2.4 Molecular Docking/Docking Simulation: Auto Dock Vina[15] was used to predict energetically favourable binding poses between the selected ligands and the carbonmonoxy Hb S protein. A total of twenty-one phytochemicals of interest were docked. The docking was executed using Local search global optimizer and implemented via the Broyden-Fletcher-Goldfarb-Shanno (BFGS) method for local optimization [15]. Validation of AutoDock Vina was carried out by redocking the co-crystallized ligand to the protein and calculating the RMSD of the docked binding pose and the crystalline binding pose. This also acted as a positive control for the docking simulations. At a docking exhaustiveness of 8, the software generated 9 poses of the protein-ligand complex which were ranked according to their binding affinity. Information on root mean standard distance (rmsd) for upper bound (rmsd u.b.) and lower bound (rmsd l.b.) of the binding poses was computed.

2.5 Analysis and Visualisation of docking simulation results: The docking poses were ranked according to their binding affinity and the conformation with the lowest binding affinity were selected for further analysis. The orientation and conformation of the binding poses, as well as the interacting residues, bond types and bond lengths were visualized with Schrödinger PyMol [19] and BIOVIA Discovery studio visualizer.

2.6: Drug Likeness and ADME analysis: Swiss ADME predictor[20] was utilized to predict the pharmacokinetic profile of the compounds of interest with top percentile binding affinity as well as a binding pose closest to that of the crystal ligand. The ligands were, also screening based on their drug likeness and lead likeness based on their compliance with Lipinski *et al*. [21], Ghose *et al*. [22], Veber *et al*. [23], Egan *et al*. [24] and Muegge *et al*. [25] filters.

3. Results

Table 1: Binding affinity of the phytochemicals of interest from GC-MS TIC of the 70% ethanolic *Zanthoxylum zanthoxyloides* stem bark extract [16]

Ligand Code	Peak Number	Retention Time	Peak Area %	IUPAC Name of Ligand (GC-MS Hit 1)	Binding Affinity of Mode 1 (Kcal/Mol)
Ligand Crystal	-	-	-	2-methyl-3-({2-[1-(propan-2-yl)-1H-pyrazol-5-yl]pyridin-3-yl}methoxy)phenol (Reference compound; co-crystallized ligand of complex 5e83)	-8.1
Ligand 1	2	4.694	0.13	Furan-2-carbaldehyde	-4.7
Ligand 2	3	6.274	0.02	5-methylfuran-2-carbaldehyde	-5.2
Ligand 3	5	8.533	0.07	(1S,5R)-6,8-dioxabicyclo[3.2.1]oct-2-en-4-one	-5.4
Ligand 4	6	9.094	0.02	3,5-dihydroxy-6-methyl-2,3-dihydropyran-4-one	-5.6
Ligand 5	10	10.338	0.32	5-(hydroxymethyl)furan-2-carbaldehyde	-5.6
Ligand 6	11	10.859	0.04	1-(2-hydroxyethyl)pyrrolidine-2,5-dione	-4.9
Ligand 7	12	11.201	0.05	3,3,4,6-tetramethyl-1-benzofuran-2-one	-7.3
Ligand 8	13	11.512	0.22	(E)-4-(1,3-benzodioxol-5-yl)but-3-en-2-one	-5.9
Ligand 9	15	11.827	0.15	1,3-benzodioxole-5-carbaldehyde	-6.1
Ligand 10	17	12.701	0.58	1-methyl-2,1-benzoxazol-3-one	-6.3
Ligand 11	18	13.842	1.41	3-ethenyl-2-methylidenecyclopentane-1-carboxylic acid	-6.2
Ligand 12	20	14.317	0.17	2-hydroxy-6-methyl-3-propan-2-ylcyclohex-2-en-1-one	-5.9
Ligand 13	21	14.380	0.29	4-hydroxy-3-methoxybenzoic acid	-6.6
Ligand 14	26	17.316	2.73	(E)-4-[4-(dimethylamino)phenyl]but-3-en-2-one	-6.4
Ligand 15	27	17.487	0.71	6,7-dimethoxychromen-2-one	-7.2
Ligand 16	29	18.500	2.00	2-[(Z)-2-nitrohept-2-enyl]cyclopentan-1-one	-6.5
Ligand 17	31	19.032	1.41	7-(dimethylamino)-2,3-dihydro-1H-cyclopenta[c]chromen-4-one	-7.8
Ligand 18	34	20.053	6.66	2,5-bis(1-adamantyl)furan	-9.6
Ligand 19	35	20.293	1.34	(8S,9S,10R,13S,14S,16R,17S)-17-acetyl-6,10,13,16-tetramethyl-8,9,11,12,14,15,16,17-octahydrocyclopenta[a]phenanthren-3-one	-9.8
Ligand 20	40	21.195	3.81	[(3S,5R,8S,9S,10R,13R,14S,17R)-5-chloro-17-[(2R,5R)-5-ethyl-6-methylheptan-2-yl]-10,13-dimethyl-1,2,3,4,6,7,8,9,11,12,14,15,16,17-tetradecahydrocyclopenta[a]phenanthren-3-yl] acetate	-8.9
Ligand 21	42	21.403	0.27	(8S)-2,6,6,9-tetramethyltricyclo[5.4.0.02,9]undecan-8-ol	-6.7

The compounds selected for molecular docking, as shown in Table 1, were pooled from the GC-MS TIC peak report of our previous study on *Z. zanthoxyloides* [16]. The compound selection was based on the presence of active functional groups which were identified from the structure-based analysis of known haemoglobin oxygen-affinity modulators. Twenty-one compounds were selected and docked on the carbonmonoxy Hb S receptor protein. Each docking run produced 9 docking conformations which were ranked according to the binding affinity using the software's default scoring function. The compounds with the strongest binding affinity were 3,3,4,6-tetramethyl-1-benzofuran-2-one (ligand 7), 6,7-dimethoxychromen-2-one (ligand 15), 7-(dimethylamino)-2,3-dihydro-1H-cyclopenta[c]chromen-4-one (ligand 17), 2,5-bis(1-adamantyl)furan (ligand 18), (8S,9S,10R,13S,14S,16R,17S)-17-acetyl-6,10,13,16-tetramethyl-8,9,11,12,14,15,16,17-octahydrocyclopenta[a]phenanthren-3-one (ligand 19) and [(3S,5R,8S,9S,10R,13R,14S,17R)-5-chloro-17-[(2R,5R)-5-ethyl-6-methylheptan-2-yl]-10,13-dimethyl-1,2,3,4,6,7,8,9,11,12,14,15,16,17-tetradecahydrocyclopenta[a]phenanthren-3-yl] acetate (ligand 20) with binding affinities of -7.3, -7.2, -7.8, -9.6, -9.8 and -8.9, respectively.

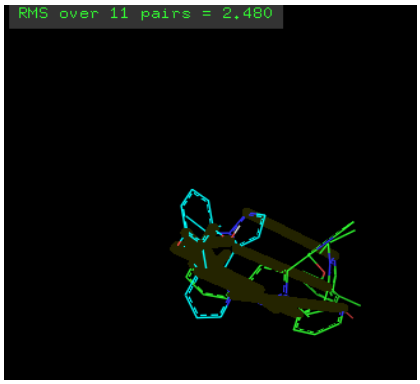

Fig 1: Pair fitting image between the x-ray crystallographic ligand pose (green structure) and *in silico* docked crystal ligand pose (blue structure). The thick dark yellow lines show the pairing between the corresponding atomic positions of the green x-ray crystallographic ligand pose and the blue *in silico* crystal ligand pose

The co-crystallized ligand, 2-methyl-3-({2-[1-(propan-2-yl)-1H-pyrazol-5-yl]pyridin-3-yl}methoxy)phenol, was re-docked with the software to validate the docking software algorithm. The RMS value of the docked conformation and the crystal structure conformation was calculated to be 2.480 Å over 11 pairs as demonstrated by Fig. 1.

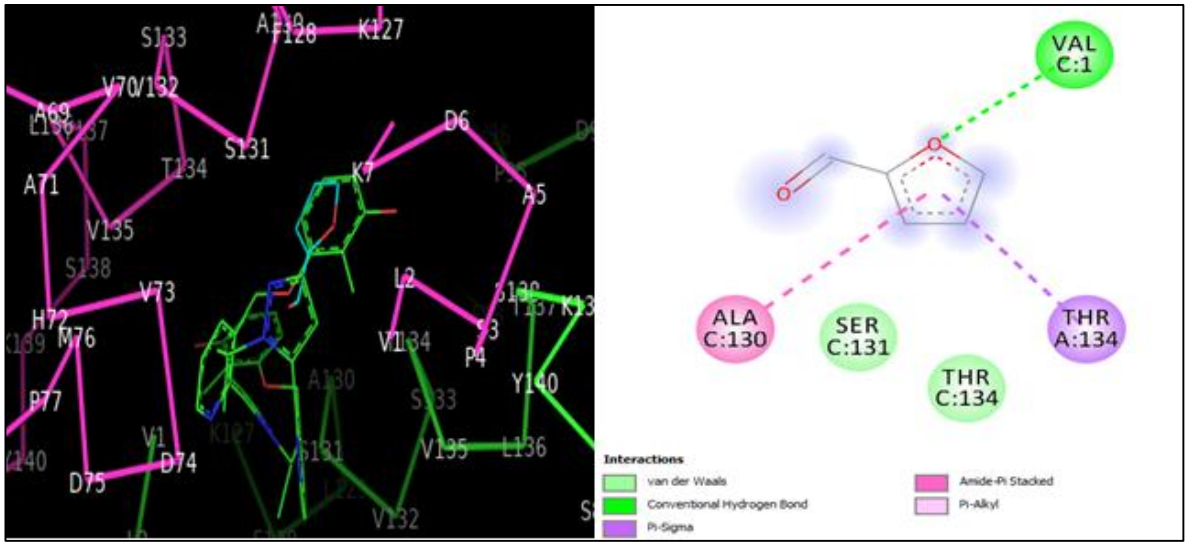

Fig 2: The image on the left compares the conformation and orientation of the crystallized binding pose of the crystal ligand (green cyclic structure) and the docked pose of furan-2-carbaldehyde (blue structure) in carbonmonoxy Hb S (the α chains are coloured purple and green while β chains are yellow and blue). Image on the right is a 2D depiction of *in silico* molecular docking interactions between furan-2-carbaldehyde and carbonmonoxy haemoglobin S

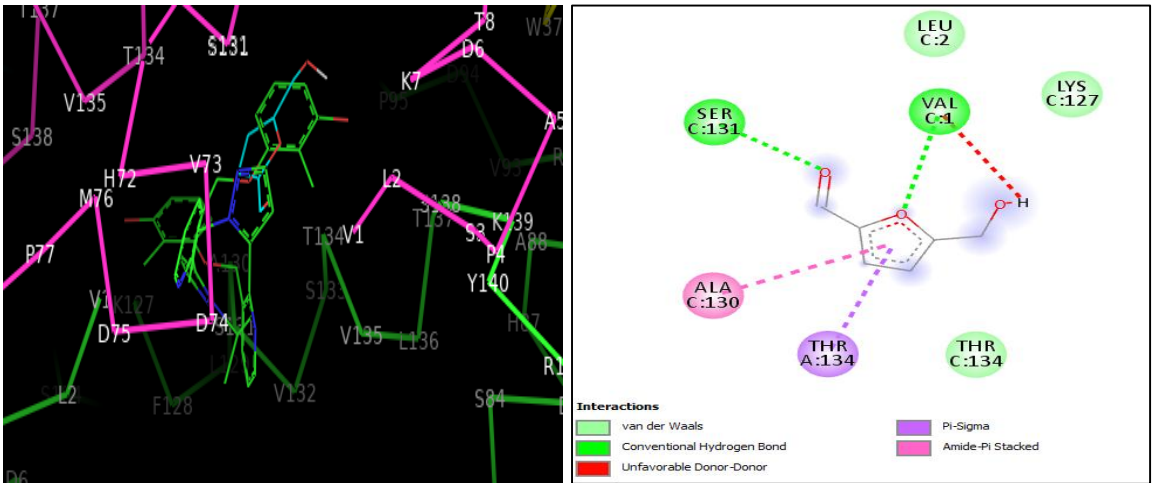

Fig 3: The image on the left compares the conformation and orientation of the crystallized binding pose of the crystal ligand (green cyclic structure) and the docked pose of 5-(hydroxymethyl) furan-2-carbaldehyde (blue structure) in carbonmonoxy Hb S (the α chains are coloured purple and green while β chains are yellow and blue). Image on the right is a 2D depiction of *in silico* molecular docking interactions between 5-(hydroxymethyl) furan-2-carbaldehyde and carbonmonoxy haemoglobin S

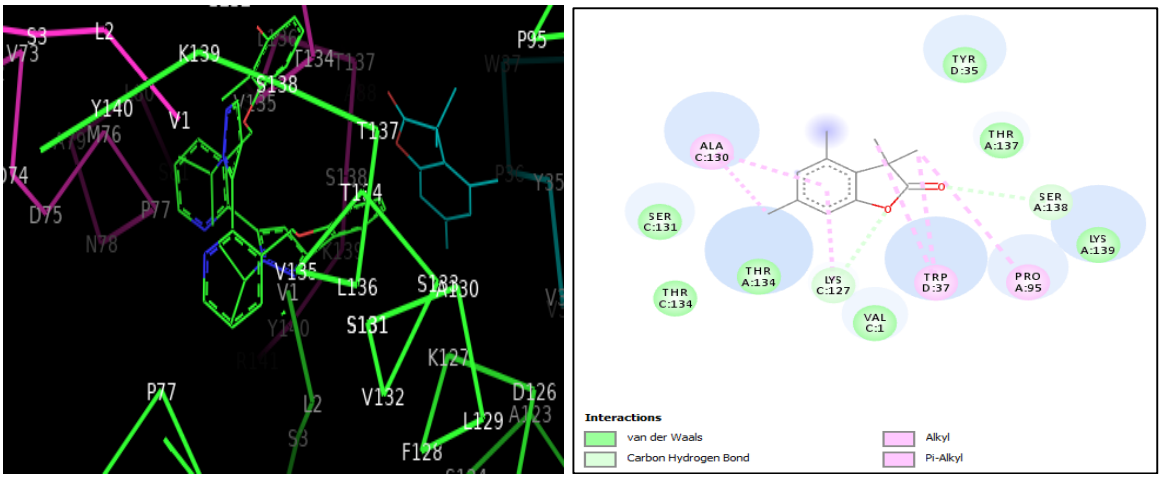

Fig 4: The image on the left compares the conformation and orientation of the crystallized binding pose of the crystal ligand (green cyclic structure) and the docked pose of 3,3,4,6-tetramethyl-1-benzofuran-2-one (blue structure) in carbonmonoxy Hb S (the α chains are coloured purple and green while β chains are yellow and blue). Image on the right is a 2D depiction of *in silico* molecular docking interactions between 3,3,4,6-tetramethyl-1-benzofuran-2-one and carbonmonoxy haemoglobin S

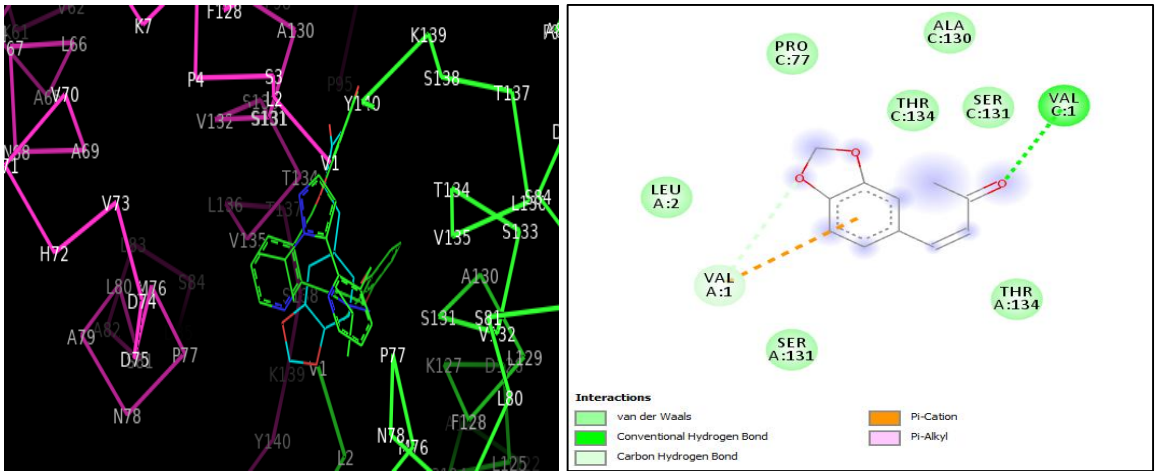

Fig 5: The image on the left compares the conformation and orientation of the crystallized binding pose of the crystal ligand (green cyclic structure) and the docked pose of (E)-4-(1,3-benzodioxol-5-yl)but-3-en-2-one (blue structure) in carbonmonoxy Hb S (the α chains are coloured purple and green while β chains are yellow and blue). Image on the right is a 2D depiction of *in silico* molecular docking interactions between (E)-4-(1,3-benzodioxol-5-yl)but-3-en-2-one and carbonmonoxy haemoglobin S

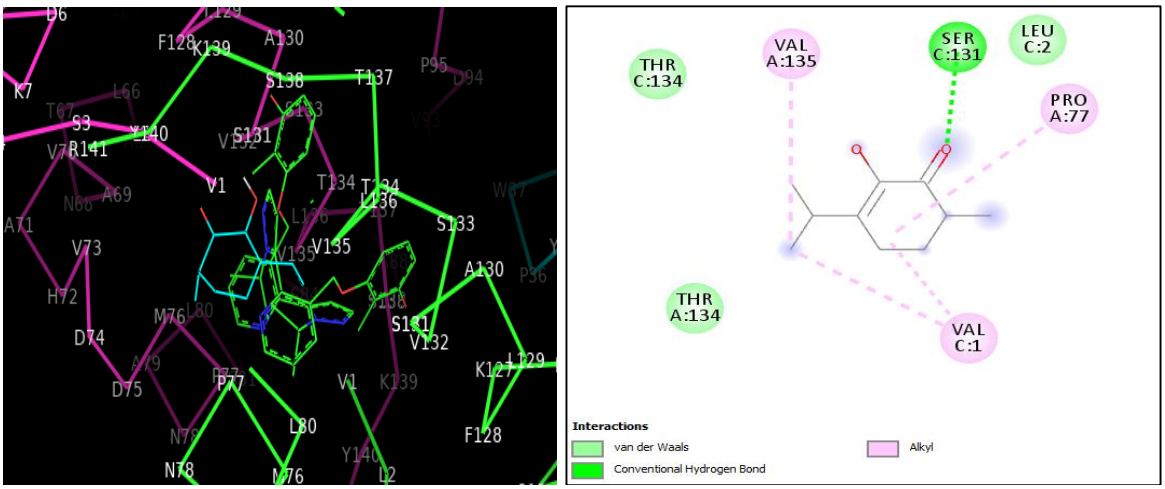

Fig 6: The image on the left compares the conformation and orientation of the crystallized binding pose of the crystal ligand (green cyclic structure) and the docked pose of 2-hydroxy-6-methyl-3-propan-2-ylcyclohex-2-en-1-one (blue structure) in carbonmonoxy Hb S (the α chains are coloured purple and green while β chains are yellow and blue). Image on the right is a 2D depiction of *in silico* molecular docking interactions between 2-hydroxy-6-methyl-3-propan-2-ylcyclohex-2-en-1-one and carbonmonoxy haemoglobin S

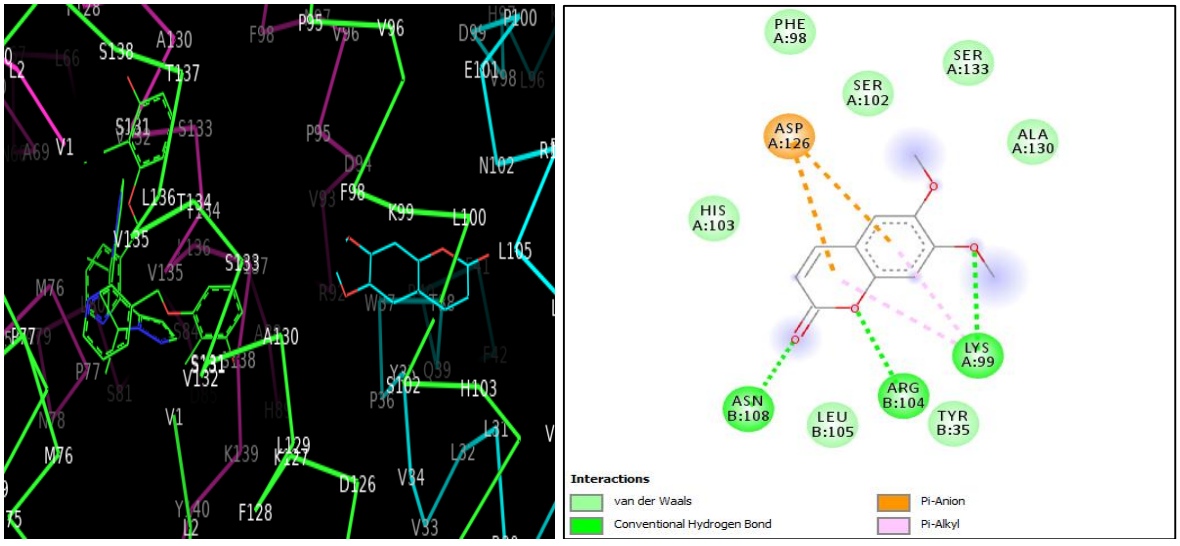

Fig 7: The image on the left compares the conformation and orientation of the crystallized binding pose of the crystal ligand (green cyclic structure) and the docked pose of 6,7-dimethoxychromen-2-one (blue structure) in carbonmonoxy Hb S (the α chains are coloured purple and green while β chains are yellow and blue). Image on the right is a 2D depiction of *in silico* molecular docking interactions between 6,7-dimethoxychromen-2-one and carbonmonoxy haemoglobin S

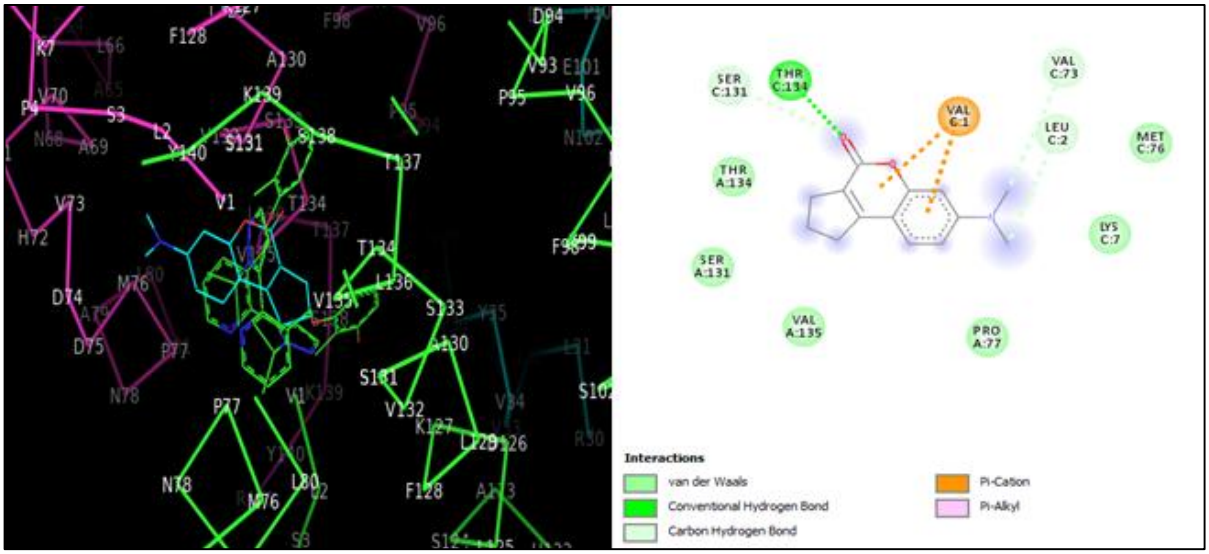

Fig 8: The image on the left compares the conformation and orientation of the crystallized binding pose of the crystal ligand (green cyclic structure) and the docked pose of 7-(dimethylamino)-2,3-dihydro-1H-cyclopenta[c]chromen-4-one (blue structure) in carbonmonoxy Hb S (the α chains are coloured purple and green while β chains are yellow and blue). Image on the right is a 2D depiction of *in silico* molecular docking interactions between 7-(dimethylamino)-2,3-dihydro-1H-cyclopenta[c]chromen-4-one and carbonmonoxy haemoglobin S

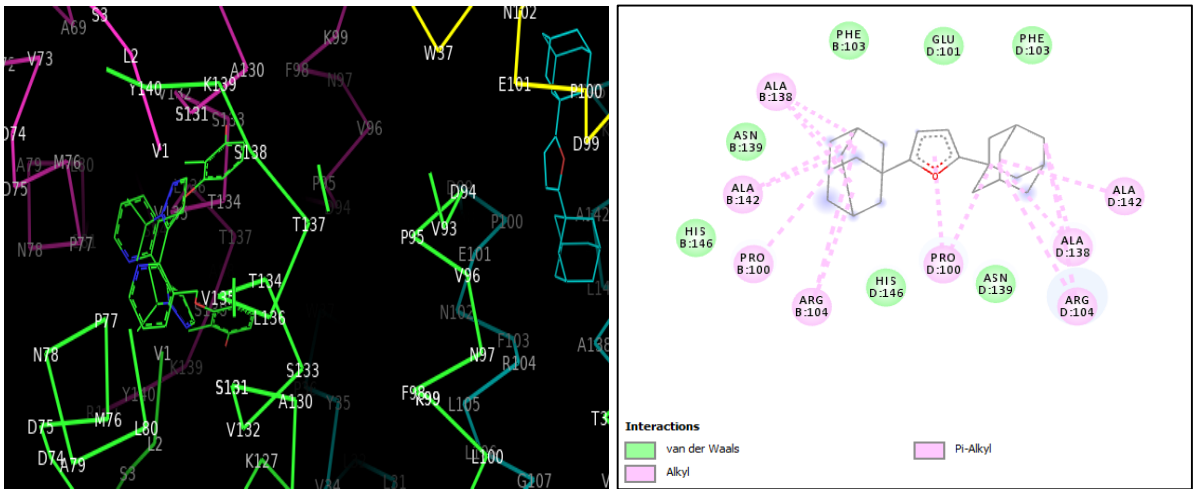

Fig 9: The image on the left compares the conformation and orientation of the crystallized binding pose of the crystal ligand (green cyclic structure) and the docked pose of 2,5-bis(1-adamantyl) furan (blue structure) in carbonmonoxy Hb S (the α chains are coloured purple and green while β chains are yellow and blue). Image on the right is a 2D depiction of *in silico* molecular docking interactions between 2,5-bis(1-adamantyl) furan and carbonmonoxy haemoglobin S

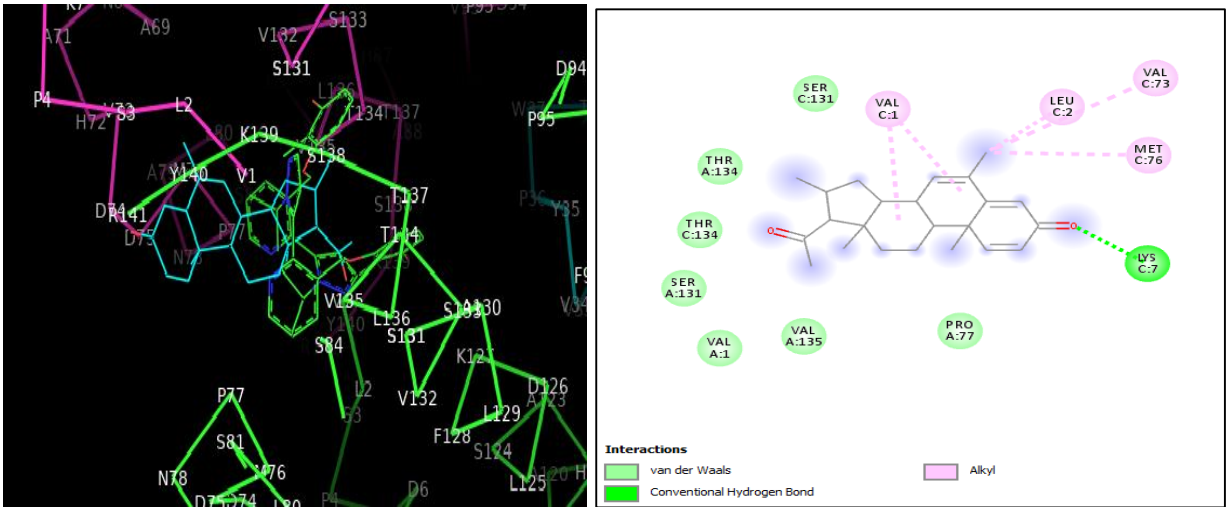

Fig 10: The image on the left compares the conformation and orientation of the crystallized binding pose of the crystal ligand (green cyclic structure) and the docked pose of (8S,9S,10R,13S,14S,16R,17S)-17-acetyl-6,10,13,16-tetramethyl-8,9,11,12,14,15,16,17-octahydrocyclopenta[a]phenanthren-3-one (blue structure) in carbonmonoxy Hb S (the α chains are coloured purple and green while β chains are yellow and blue). Image on the right is a 2D depiction of *in silico* molecular docking interactions between (8S,9S,10R,13S,14S,16R,17S)-17-acetyl-6,10,13,16-tetramethyl-8,9,11,12,14,15,16,17-octahydrocyclopenta[a]phenanthren-3-one and carbonmonoxy haemoglobin S

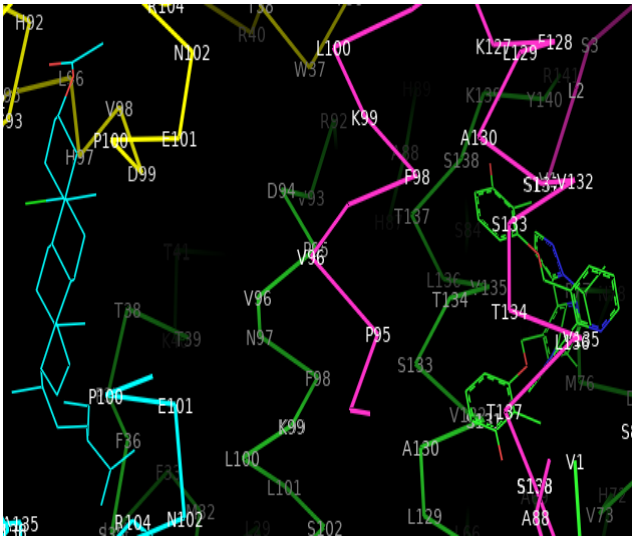

Fig 11: The image compares the conformation and orientation of the crystallized binding pose of the crystal ligand (green cyclic structure) and the docked pose of [(3S,5R,8S,9S,10R,13R,14S,17R)-5-chloro-17-[(2R,5R)-5-ethyl-6-methylheptan-2-yl]-10,13-dimethyl-1,2,3,4,6,7,8,9,11,12,14,15,16,17-tetradecahydrocyclopenta[a]phenanthren-3-yl] acetate (blue structure) in carbonmonoxy Hb S (the α chains are coloured purple and green while β chains are yellow and blue)

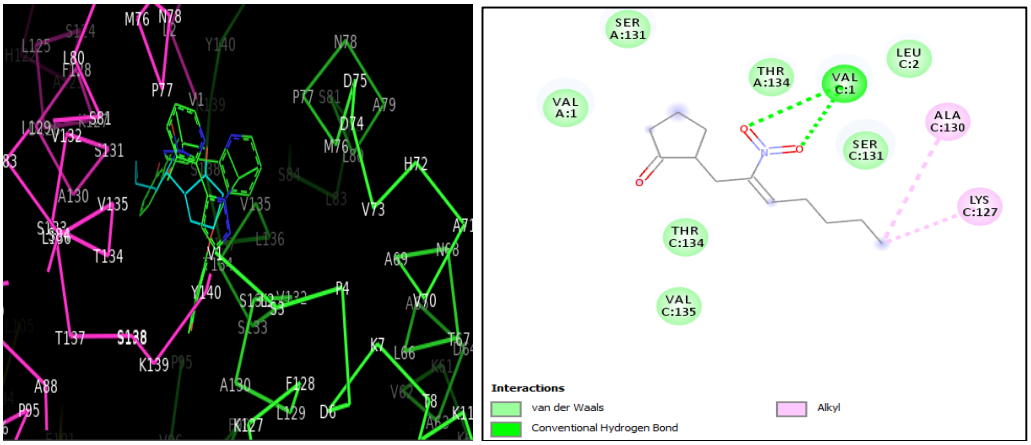

Fig 12: The image on the left compares the conformation and orientation of the crystallized binding pose of the crystal ligand (green cyclic structure) and the docked pose of 2-[(Z)-2-nitrohept-2-enyl]cyclopentan-1-one (blue structure) in carbonmonoxy Hb S (the α chains are coloured purple and green while β chains are yellow and blue). Image on the right is a 2D depiction of *in silico* molecular docking interactions between 2-[(Z)-2-nitrohept-2-enyl]cyclopentan-1-one and carbonmonoxy haemoglobin S

Out of the twenty-one ligands docked, seven ligands had binding poses most similar to that of the crystal pose. The seven with the closest binding poses were furan-2-carbaldehyde (ligand 1), 5-(hydroxymethyl)furan-2-carbaldehyde (ligand 5), (E)-4-(1,3-benzodioxol-5-yl)but-3-en-2-one (ligand 8), 2-hydroxy-6-methyl-3-propan-2-ylcyclohex-2-en-1-one (ligand 12), 7-(dimethylamino)-2,3-dihydro-1H-cyclopenta[c]chromen-4-one (ligand 17), (8S,9S,10R,13S,14S,16R,17S)-17-acetyl-6,10,13,16-tetramethyl-8,9,11,12,14,15,16,17-octahydrocyclopenta[a]phenanthren-3-one (ligand 19) and 2-[(Z)-2-nitrohept-2-enyl]cyclopentan-1-one (ligand 16).

Eleven docking poses, representing ligands with the strongest binding affinity and with a binding pose most similar to the crystallized pose, were further analysed. The Fig. 2-12 show the interaction between the selected eleven bioactive phytochemical ligands and the carbonmonoxy Hb S receptor protein.

Furan-2-carbaldehyde with binding affinity of -4.7 showed hydrogen bond, pi-sigma, amide-pi stacked and van der Waals interactions with alpha chain residues; valine C:1, threonine A:134, alanine C:130, serine C:131 and threonine C:134 as in Fig. 2.

5-(hydroxymethyl)furan-2-carbaldehyde with binding affinity of -5.6 showed hydrogen bond, pi-sigma, amide-pi stacked, van der Waals and unfavourable donor-donor interactions with alpha chain residues; valine C:1, serine C:131, threonine A:134, alanine C:130, leucine C:2, lysine C:127 and threonine C:134 as in Fig. 3.

3,3,4,6-tetramethyl-1-benzofuran-2-one with binding affinity of -7.3 showed alkyl, pi-alkyl, carbon hydrogen bond and van der Waals interactions with alpha and beta chain residues; tryptophan D:35, threonine A:137, serine A:138, lysine A:139, proline A:95, tryptophan D:37, valine C:1, alanine C:130, lysine C:127, threonine C:134, serine C:131 and threonine A:134 as in Fig. 4.

(E)-4-(1,3-benzodioxol-5-yl)but-3-en-2-one with binding affinity of -5.9 showed hydrogen bond, pi-cation, van der Waals, interactions with alpha chain residues; valine C:1, valine A:1, serine A:131, threonine A:134, alanine C:130, proline C:77, leucine A:2, serine C:131 and threonine C:134 as in Fig. 5.

2-hydroxy-6-methyl-3-propan-2-ylcyclohex-2-en-1-one with binding affinity of -5.9 stabilized by hydrogen bonds, alkyl and van der Waals interactions with alpha chain residues; serine C:131, valine A:135, proline A:77, valine C:1, threonine C:134, threonine A:134 and leucine C:2 as in Fig. 6.

6,7-dimethoxychromen-2-one with binding affinity of -7.2 showed hydrogen bonds, pi-anion. pi-alkyl and van der Waals interactions with alpha and beta globin residues; asparagine B:108, arginine B:104, lysine A:99, aspartic acid A:126, serine A:102, serine A:133, phenylalanine A:98, alanine A:130, histidine A:103, leucine B:105 and tyrosine B:35 as in Fig. 7.

7-(dimethylamino)-2,3-dihydro-1H-cyclopenta[c]chromen-4-one with binding affinity of-7.8 showed hydrogen bond, pi-cation, carbon hydrogen bond and van der Waals interactions with alpha globin residues; threonine C:134, valine C:1, serine C:131, valine C:73, leucine C:2, threonine A:134, serine A:131, valine A:135, proline A:77, lysine C:7 and methionine C:76 as in Fig. 8.

2,5-bis(1-adamantyl)furan with binding affinity of -9.6 demonstrated pi-alkyl, alkyl and van der Waals interactions with beta globin residues; proline D:100, alanine D:142, alanine D:138, arginine D:104, asparagine D:139, histidine D:146, arginine B:104, proline B:100, histidine B:146, alanine B:142, asparagine B:139, alanine B:138, phenylalanine B:103, glutamic acid D:101 and phenylalanine D:103 as in Fig. 9.

(8S,9S,10R,13S,14S,16R,17S)-17-acetyl-6,10,13,16-tetramethyl-8,9,11,12,14,15,16,17-octahydrocyclopenta[a]phenanthren-3-one with binding affinity of -9.8 demonstrated hydrogen bond, alkyl and van der Waals interactions with alpha globin residues; lysine C:7, methionine C:76, valine C:73, leucine C:2, valine C:1, serine C:131, threonine A:134, threonine C:134, serine A:131, valine A:1, valine A:135 and proline A:77 as in Fig. 10.

[(3S,5R,8S,9S,10R,13R,14S,17R)-5-chloro-17-[(2R,5R)-5-ethyl-6-methylheptan-2-yl]-10,13-dimethyl-1,2,3,4,6,7,8,9,11,12,14,15,16,17-tetradecahydrocyclopenta[a]phenanthren-3-yl] acetate with binding affinity of -8.9 as in Fig. 11. However, we are unable to generate the 2D ligand receptor interaction image to view the interacting residues and bond types using BIOVIA Discovery studio visualizer. Visualization with PyMol showed a polar interaction with beta globin residue, alanine D:135 at a site somewhat distant from the crystal binding site.

2-[(Z)-2-nitrohept-2-enyl]cyclopentan-1-one with binding affinity of -6.5 showed hydrogen bond, alkyl and van der Waals interactions with alpha chain residues valine C:1, alanine C:130, lysine C:127, leucine C:2, serine C:131, threonine A:134, threonine C:134, valine C:135, valine A:1 and serine A:131 as in Fig. 12.

Table 2: ADME profile of 7-(dimethylamino)-2,3-dihydro-1H-cyclopenta[c]chromen-4-one and (8S,9S,10R,13S,14S,16R,17S)-17-acetyl-6,10,13,16-tetramethyl-8,9,11,12,14,15,16,17-octahydrocyclopenta[a]phenanthren-3-one

S/N	ADME Parameter	Compound Name	
		7-(dimethylamino)-2,3-dihydro-1H-cyclopenta[c]chromen-4-one	**(8S,9S,10R,13S,14S,16R,17S)-17-acetyl-6,10,13,16-tetramethyl-8,9,11,12,14,15,16,17-octahydrocyclopenta[a]phenanthren-3-one**
Physiochemical Properties			
1.	Formula	C14H15NO2	C23H30O2
2.	Molecular weight	229.27 g/mol	338.48 g/mol
3.	Number of rotatable bonds	1	1
4.	Number of H-bond acceptors	3	2
5.	Number of H-bond donors	0	0
6.	Molar refractivity	69.32	102.68
7.	TPSA	33.45 Å^2	34.14 Å^2
Lipophilicity			
8.	Log Po/w (iLOGP)	2.57	3.35
9.	Log Po/w (XLOGP3)	2.43	4.34
10.	Log Po/w (WLOGP)	2.35	4.91
11.	Log Po/w (MLOGP)	2.45	4.21
12.	Log Po/w (SILICOS-IT)	3.17	4.28
13.	Lipophilicity (Consensus Log P $_{o/w}$)	2.59	4.22
Water Solubility			
14.	Log S (ESOL) Solubility class	-3.16 Soluble	-4.61 Moderately soluble
15.	Log S (Ali) Solubility class	-2.78 Soluble	-4.77 Moderately soluble
16.	Log S (SILICOS-IT) Solubility class	-4.56 Moderately soluble	-4.20 Moderately soluble
Druglikeness, Leadlikeness and Medicinal Chemistry			
17.	Lipinski	No violations	1 violation: MLOGP>4.15
18.	Ghose	No violations	No violations
19.	Veber	No violations	No violations
20.	Egan	No violations	No violations
21.	Muegge	No violations	No violations
22.	Bioavailability score	0.55	0.55
23.	Lead likeness	1 violation (MW<250)	1 violation (XLOGP3>3.5)
24.	Synthetic accessibility	3.11	5.63

Pharmacokinetic Properties			
25.	GI absorption	High	High
26.	BBB permeant	Yes	Yes
27.	P-gp substrate	No	No
28.	CYP1A2 inhibitor	Yes	No
29.	CYP2C19 inhibitor	No	Yes
30.	CYP2C9 inhibitor	No	Yes
31.	CYP2D6 inhibitor	No	No
32.	CYP3A4 inhibitor	No	No

The compounds, 7-(dimethylamino)-2,3-dihydro-1H-cyclopenta[c]chromen-4-one and (8S,9S,10R,13S,14S,16R,17S)-17-acetyl-6,10,13,16-tetramethyl-8,9,11,12,14,15,16,17-octahydrocyclopenta[a]phenanthren-3-one, demonstrated good compliance with the drug likeness filters. They were predicted to possess high gastro-intestinal absorption and a bioavailability score of 0.55.

4. Discussion

Zanthoxylum zanthoxyloides has been historically used in the management of sickle cell anemia, particularly in African traditional medicine. Over the years, there has been a resurgence in its use, largely due to the lack of therapeutic options, inadequate control of the disorder symptoms and limitations associated with approved therapies for sickle cell anemia. Before the approval of Voxelotor and Crizanlizumab in 2019 and Endari in 2017, the only FDA approved medicine for sickle cell treatment for patients aged five and older was Hydroxyurea which was approved almost 20 years ago; underlining the obvious dearth of approved therapeutic options and the sluggish rate of approval of new medicines for this disorder.

Previous studies in sickle cell anemia utilizing biophysical tools such as x-ray crystallography and nuclear magnetic resonance spectroscopy have elucidated at a molecular level the mechanism of action of several active compounds that inhibit Hb S polymerization through haemoglobin oxygen-affinity modulation [13, 26]. With the integration of computational protocols in this study, we delved into a preliminary *in silico* evaluation of *Zanthoxylum zanthoxyloides*.

4.1 *In silico* molecular docking studies

The significant binding pose similarity between the x-ray crystallographic ligand conformation and the *in silico* crystal ligand conformation suggested good reliability and reproducibility of the software. The binding pose reproduction quality was quantified using the root mean square deviation (RMSD) value. The pair fitting wizard of PyMol [19] was utilized to calculate the RMS value of the poses as shown in Fig. 1. With an RMS of 2.480 Å over 11 corresponding atomic pairs spread over the entire ligand structure, an acceptable reproduction of the crystallographic binding pose was observed. In this study, RMSD values less than 2.0 Å were classified as good, 2.0 Å to 3.0 Å are acceptable while values >3 Å are unacceptable [27].

The selection criteria for the ligands studied was based on a structure-activity analysis of known compounds with haemoglobin oxygen-affinity modulatory activity. The presence of certain functional groups has been suggested to be an important chemical property of haemoglobin oxygen-affinity modulators. A classic example are the aromatic aldehydes and their derivatives such as vanillin, 5-hydroxymethyl-2-furfural and the International Nonproprietary Name (INN) compounds; Tucaresol, and Valeresol. These compounds possess the capability to form multiple interactions including the Schiff-base adduct with the Hb S α-globin N-terminal valine[8]. Thus, compounds selected for docking were assessed for the presence of active functional groups such as the carbonyl, ether and aromatic ring system.

The molecular interactions of the x-ray crystallographic image of the liganded carbonmonoxy Hb S complex has been described by Oksenberg *et al* [13]. Interactions involved in the stabilization of the complex include a reversible Schiff base covalent bond with the N-terminal α-chain residue, valine A:1 or valine C:1 and a hydrogen bond with serine A:131 or serine C:131 on the adjacent α-chain. Whilst the involvement of hydrophobic contacts, pi, alkyl and other intermolecular interactions were not mentioned in the study, these bond types are energetically relevant in ligand-receptor binding. Thus, the involvement of other spatially close residues is theoretically possible.

From the pool of docked ligands with the strongest binding affinity and a docking pose at the literature\crystallographic binding site with interaction patterns similar to that of the crystal pose, two compounds; 7-(dimethylamino)-2,3-dihydro-1H-cyclopenta[c]chromen-4-one and (8S,9S,10R,13S,14S,16R,17S)-17-acetyl-6,10,13,16-tetramethyl-8,9,11,12,14,15,16,17-octahydrocyclopenta[a]phenanthren-3-one intersected the two sets, having binding affinities of -7.8 and -9.8 respectively and a binding pose similar to the crystal pose.

In comparison with the crystal ligand, the coumarin, 7-(dimethylamino)-2,3-dihydro-1H-cyclopenta[c]chromen-4-one formed interactions with valine C:1 and serine A:131 as shown in Fig. 8. A hydrogen bond with threonine C:134, between the carbonyl O2 atom of the coumarin and the hydrogen atom of the hydroxyl group of threonine C:134 with a bond length of 2.6 Å, was implicated. Three carbon-hydrogen bonds, a weaker type of hydrogen bond, involving hydrogen atoms attached to a carbon atom linked to an electronegative atom were shown to play a role. The binding pose was also stabilized by a strong pi-cation interaction, a major force of molecular recognition energetically significant in biological systems [28]. This was formed between the terminal amino group of Valine C:1, which undergoes protonation to form a cation under physiological conditions, and the pi system of the ligand. Other intermolecular forces include the comparatively weaker van der Waal interactions.

As shown in Fig. 10, the phytosterol, (8S,9S,10R,13S,14S,16R,17S)-17-acetyl-6,10,13,16-tetramethyl-8,9,11,12,14,15,16,17-octahydrocyclopenta[a]phenanthren-3-one interacted with valine C:1, valine A:1 and serine A:131, in similarity with the crystal pose. A hydrogen bond between oxygen O2 of the ligand carbonyl group and the hydrogen of the amine group of lysine C:7 residue with a bond length 2.3 Å, was shown to be involved. The docking was also stabilized by important relatively high energy hydrophobic alkyl interactions between alkyl groups of the hydrophobic amino acids; valine C:1, leucine C:2, valine C:73 and methionine C:76 and the ligand alkyl groups. Val der Waal interactions were demonstrated to play a role in the stabilization of this interaction.

In summary, two phytochemical constituents exhibited a strong binding affinity, a similar binding pose and interaction pattern to the crystal ligand-protein complex[13]. This evidence suggests a potential of these two compounds to elicit a similar haemoglobin oxygen-affinity modulatory action and thus, provides an alternative mode of action for the reported therapeutic effects of *Zanthoxylum zanthoxyloides* in sickle cell anemia. Confirmation of this activity through x-ray crystallography, surface plasmon resonance and transgenic mice experimental designs is important to confirm a preferential stability of the high oxygen-affinity (R-state) Hb S over low oxygen-affinity (T-state) Hb S.

4.2 ADME profile of anti-sickling compounds of interest

The ADME properties of a biologically active compound refer to its pharmacokinetic parameters; absorption, distribution, metabolism and excretion and is strongly related to its physiochemical properties. These parameters are important and determine a compound's bioavailability, pharmacokinetic and toxicity profile. In drug discovery and development, it is imperative to consider ADMET properties early in the drug development cycle to prevent late stage failure of potential medicines. Here, computational ADME predictors serve as valuable guides.

7-(dimethylamino)-2,3-dihydro-1H-cyclopenta[c]chromen-4-one belongs to a class of organic compounds known as coumarins, which are a family of benzopyrone with a unifying lactone functional group. While (8S,9S,10R,13S,14S,16R,17S)-17-acetyl-6,10,13,16-tetramethyl-8,9,11,12,14,15,16,17-octahydrocyclopenta[a]phenanthren-3-one, a phytosterol, possesses the heterocyclic steroidal skeleton which is composed of three 6-membered cyclohexane and a 5-membered cyclopentane ring.

Using data from Swiss ADME and PubChem, the drug- and lead- likeness of these two compounds were assessed by considering the compliance of their physicochemical properties with limits specified on five predictive filters: Lipinski *et al*., Ghose *et al*., Veber *et al*., Egan *et al*. and Muegge *et al*. The specified limits of these filters are based on the analysis of the physiochemical properties of successful oral drug molecules, which highlighted important influencing physiochemical properties such as molecular mass, log P, molar refractivity, number of rotatable bonds, topological polar surface area, number hydrogen bond acceptors and hydrogen bond donor as key determinants. 7-(dimethylamino)-2,3-dihydro-1H-cyclopenta[c]chromen-4-one had excellent compliance with the filters; there were no violations. The phytosterol had one violation. The MLOGP at 4.21 was greater than the upper limit of 4.15. MLOGP is a measure of the lipophilicity of the compound and has a direct proportionality to its lipophilicity. In essence, the higher the MLOGP, the greater the lipophilicity. While it is important for a potential drug molecule to be lipophilic enough to partition into the lipid bilayer during absorption, it is crucial that it is not too lipophilic, where its movement through the biological interface will be hindered and accumulation in hydrophobic storage tissues will be facilitated.

The two compounds exhibited violations in the lead-likeness assessment. The importance of lead-likeness is evident in the process of chemical optimization of potential medicines to improve their pharmacodynamic and pharmacokinetic properties. 7-(dimethylamino)-2,3-dihydro-1H-cyclopenta[c]chromen-4-one had a violation in its molecular weight while (8S,9S,10R,13S,14S,16R,17S)-17-acetyl-6,10,13,16-tetramethyl-8,9,11,12,14,15,16,17-octahydrocyclopenta[a]phenanthren-3-one had a violation in its lipophilicity.

The two compounds were predicted to possess a high intestinal absorption, the ability to permeate the blood brain barrier (BBB) and a bioavailability score of 0.55. They were also predicted not to be permeability glycoprotein (P-gp) substrates. This suggest the feasibility of the oral route of administration and supports the reported oral administration of *Z. zanthoxyloides* infusions/extracts/decoction in traditional medicine. The ability and extent of BBB permeation may confer a neurological effect to the compounds. In regards to their influence on cytochrome P450 enzymes which are responsible for the metabolism of a wide variety of substrates including xenobiotics, 7-(dimethylamino)-2,3-dihydro-1H-cyclopenta[c]chromen-4-one was predicted to be a CYP1A2 inhibitor while (8S,9S,10R,13S,14S,16R,17S)-17-acetyl-6,10,13,16-tetramethyl-8,9,11,12,14,15,16,17-octahydrocyclopenta[a]phenanthren-3-one, a CYP2C19 inhibitor and CYP2C9 inhibitor. The inhibition of these enzymes will inform the co-administration of *Zanthoxylum zanthoxyloides* products with exogenous substances including other medicines.

5. Conclusion

The findings from the *in silico* evaluation of the chemical constituents of *Zanthoxylum zanthoxyloides* stem bark identifies two compounds, 7-(dimethylamino)-2,3-dihydro-1H-cyclopenta[c]chromen-4-one and (8S,9S,10R,13S,14S,16R,17S)-17-acetyl-6,10,13,16-tetramethyl-8,9,11,12,14,15,16,17-octahydrocyclopenta[a]phenanthren-3-one, discovered to possess a strong binding affinity comparable to that of the crystal ligand for a binding pocket on Hb S associated with haemoglobin oxygen-affinity modulatory activity. This is a novel report of haemoglobin oxygen-affinity modulatory action for these phytochemicals and the *Zanthoxylum zanthoxyloides* plant. The compounds exhibited an interaction pattern similar to the crystal ligand and other compounds that have been reported to possess haemoglobin oxygen-affinity modulatory activity. The compounds, also, demonstrated a favourable predicted pharmacokinetic, drug likeness and lead likeness profile. The sum of this investigation provides a foundation for further experimental inquiry to validate the activity and potency of the bioactive phytochemicals of *Zanthoxylum zanthoxyloides* as haemoglobin oxygen-affinity modulators.

Competing interests: The authors declare that they have no competing interests.

Acknowledgements

The authors acknowledge the Federal Institute of Industrial Research, Oshodi, Lagos, Nigeria for the infrastructural and financial support of this study. No other funding grants were obtained elsewhere.

Author's Contributions: AAO, UEI, GA, IAD and CCI contributed to the study conception and design. AAO performed the molecular docking and ADME computational analyses. The first draft of the manuscript was written by AAO and all authors commented on previous versions of the manuscript. All authors read and approved the final manuscript.

6. References

1. Grosse SD, Odame I, Atrash HK, Amendah DD, Piel FB, Williams TN. Sickle cell disease in Africa: a neglected cause of early childhood mortality. Am J Prev Med 2011;41(6 suppl4):S398-S405. https://doi.org/10.1016/j.amepre.2011.09.013
2. Agrawal RK, Patel RK, Shah V, Nainiwal L, Trivedi B. Hydroxyurea in sickle cell disease: drug review. Indian J Hematol Blood Transfus 2014;30(20):91-96. https://doi.org/10.1007/s12288-013-0261-4
3. Field JJ, Nathan DG, Linden J. The role of adenosine signalling in sickle cell therapeutics. Hematol Oncol Clin North Am 2014;28(2):287-299. https://doi.org/10.1016/j.hoc.2013.11.003
4. Quinn CT. L-glutamine for sickle cell anemia: more questions than answers. Blood 2018;132(7):689-693. https://doi.org/10.1182/blood-2018-03-834440
5. Armstrong Madeleine. Global Blood aims for sickle cell dominance. Vantage. 2018. https://www.evaluate.com/vantage/articles/events/company-events/global-blood-aims-sickle-cell-dominance. Accessed 25 June 2019
6. Ataga KI, Desai PC. Advances in new drug therapies for the management of sickle cell disease. Expert Opin Orphan D 2018;6(5):329-343. https://doi.org/10.1080/21678707.2018.1471983
7. Nurain IO, Bewaji CO, Johnson JS, Davenport RD, Zhang Y. Potential of Three Ethnomedicinal Plants as Antisickling Agents. Mol Pharm 2017;14(1):172-182. https://doi.org/10.1021/acs.molpharmaceut.6b00767
8. Xu GG, Pagare PP, Ghatge MS, Safo RP, Gazi A, Chen Q *et al*. Design, synthesis, and biological evaluation of ester and ether derivatives of antisickling agent 5-HMF for the treatment of sickle cell disease. Mol Pharm 2017;14(10):3499-3511. https://doi.org/10.1021/acs.molpharmaceut.7b00553
9. Matu EN. *Zanthoxylum zanthoxyloides* (Lam.) Zepern. & Timler. In: Schmelzer GH, Gurib-Fakim A (eds) PROTA (Plant Resources of Tropical Africa / Ressources végétales de l'Afrique tropicale). Wageningen, Netherlands 2011. https://www.prota4u.org/database/protav8.asp?g=pe&p=Zanthoxylum+zanthoxyloides+(Lam.)+Zepern.+&+Timler. Accessed 11 April 2019
10. Ouattara B, Angenota L, Guissou P, Fondu P, Dubois J, Frédérich M *et al*. LC/MS/NMR analysis of isomeric divanilloylquinic acids from the root bark of *Fagara zanthoxyloides* Lam. Phytochemistry 2004;65(8):1145-1151. https://doi.org/10.1016/j.phytochem.2004.02.025
11. Ouattara B, Jansen O, Angenot L, Guissou IP, Frédérich M, Fondud P *et al*. Antisickling properties of divanilloylquinic acids isolated from *Fagara zanthoxyloides* Lam. (Rutaceae). Phytomedicine 2009;16(2, 3):125-129. https://doi.org/10.1016/j.phymed.2008.10.013
12. Adesina SK. The Nigerian Xanthoxylum; chemical and biological values. AJTCAM 2005;2(3):282-301
13. Oksenberg D, Dufu K, Patel MP, Chuang C, Li Z, Xu Q *et al*. GBT440 increases haemoglobin oxygen affinity, reduces sickling and prolongs RBC half-life in a murine model of sickle cell disease. Br J Haematol 2016;175:141-153 PDB ID:5E83
14. Dassault Systemes BIOVIA. Discovery Studio Modelling Environment, Release 2017. Dassault Systemes: San Diego 2016.
15. Trott O, Olson AJ. AutoDock Vina: improving the speed and accuracy of docking with a new scoring function, efficient optimization and multithreading. J Comput Chem 2010;31:455-461
16. Olushola-Siedoks AA, Igbo UE, Asieba G, Damola IA, Igwe CC. Elemental analysis and phytochemical characterisation of *Zanthoxylum zanthoxyloides* (Lam.) Zepern. and Timler stem bark. J Phar. J Pharmacogn Phytochem 2020;9(5):41-46. https://doi.org/10.22271/phyto.2020.v9.i5a.12420
17. Kim S, Chen J, Cheng T, Gindulyte A, He J, He S *et al*. PubChem 2019 update: improved access to chemical data. Nucleic Acids Res 2019;47(D1):D1102-1109. https://doi.org/10.1093/nar/gky1033 [PubMed PMID: 30371825]
18. Pettersen EF, Goddard TD, Huang CC, Couch GS, Greenblatt DM, Meng EC *et al*. UCSF Chimera--a visualization system for exploratory research and analysis. J Comput Chem 2004;25(13):1605-12
19. The PyMOL Molecular Graphics System, Version 2.0 Schrödinger, LLC
20. Daina A, Michielin O, Zoete V. SwissADME: a free web tool to evaluate pharmacokinetics, drug-likeness and medicinal chemistry friendliness of small molecules. Sci Rep 2017;7:42717
21. Lipinski CA, Lombardo F, Dominy BW, Feeney PJ. Experimental and computational approaches to estimate solubility and permeability in drug discovery and development settings. Adv Drug Deliv Rev 2001;46(1-3):3-26. https://doi.org/10.1016/s0169-409x(00)00129-0
22. Ghose AK, Viswanadhan VN, Wendoloski JJ. A knowledge-based approach in designing combinatorial or medicinal chemistry libraries for drug discovery. 1. A qualitative and quantitative characterization of known drug databases. J Comb Chem 1999;1:55-68. https://doi.org/10.1021/cc9800071
23. Veber DF, Johnson SR, Cheng HY, Smith BR, Ward KW, Kopple KD. Molecular properties that influence the oral bioavailability of drug candidates. J Med Chem 2002;45:2615-2623. https://doi.org/10.1021/jm020017n
24. Egan WJ, Merz KM, Baldwin JJ. Prediction of drug absorption using multivariate statistics. J Med Chem 2000;43:3867-3877. https://doi.org/10.1021/jm000292e
25. Muegge I, Heald SL, Brittelli D. Simple selection criteria for drug-like chemical matter. J Med Chem 2001;44:1841-1846. https://doi.org/10.1021/jm015507e
26. Pagare PP, Ghatge MS, Musayev FN, Deshpande TM, Chen Q, Braxton C *et al*. Rational design of pyridyl derivatives of vanillin for the treatment of sickle cell disease. Bioorgan Med Chem 2018;26(9):2530-2538.
27. Ramirez D, Caballero J. Is it reliable to take the molecular docking top scoring position as the best solution without considering available structural data? Molecules 2018;23(5):1038. https://doi.org/10.3390/molecules23051038
28. Dougherty DA. The Cation−π Interaction. Acc Chem Res 2013;46(4):885-893. https://doi.org/10.1021/ar300265y